Full band Monte Carlo simulations of high-field electron transport in GaAs and ZnS

Niels Fitzer, Angelika Kuligk and Ronald Redmer
Fachbereich Physik, Universität Rostock, D-18051 Rostock, Germany

Martin Städele
Infineon Technologies AG, Corporate Research ND, Otto-Hahn-Ring 6, D-81730 München, Germany

Stephen M. Goodnick
Department of Electrical Engineering, Arizona State University, Tempe, AZ 85287-5706, USA

Wolfgang Schattke
Institut für Theoretische Physik,
Christian-Albrechts-Universität Kiel, Leibnizstraße 15,
D-24118 Kiel, Germany

(Dated: February 28, 2003)

We study the high field transport in GaAs and ZnS based on *ab initio* band structures determined within density functional theory using an exact exchange formalism with a local density approximation for correlations. The transport properties are gained from ensemble Monte Carlo simulations where all relevant scattering mechanisms are considered including a realistic impact ionization rate. New results are shown for the drift velocity, the mean kinetic energy, and the valley occupation.

PACS numbers: 71.15.Mb, 71.55.Eq, 71.55.Gs, 72.20.Ht, 72.80.Ey

Introduction.– High field transport in semiconductors is of fundamental theoretical interest and has wide practical applications [1]. Besides Si as the most common semiconductor material, GaAs is of relevance for, e.g., optoelectronic devices. The properties of wide band gap materials such as ZnS, GaN, and SrS are needed to, e.g., design efficient electroluminescent displays.

Electron transport in such semiconductor materials is usually described by means of simulation techniques such as the ensemble Monte Carlo method [2, 3] or the cellular-automaton method [4]. The microscopic scattering rates and the full band structure in the entire Brillouin zone are needed in these formalisms. We have performed *ab initio* band structure calculations for GaAs and ZnS within density functional theory (DFT) using an exact exchange formalism with a local density approximation for correlations (EXX-LDA) [5]. The exact treatment of the exchange interaction allows one to reproduce band gap energies very accurately for a variety of semiconductor materials, in contrast to the LDA which is plagued by the well-known band gap problem [6]. Therefore, strongly improved *ab initio* band structures are now available for the description of excitation and transport processes in semiconductors.

The transport properties are gained from ensemble Monte Carlo simulations where, besides the various electron-phonon scattering processes, also a realistic impact ionization rate is considered. The latter process becomes important for high field strengths where *hot* conduction band electrons can impact ionize valence band electrons and, thus, lead to carrier multiplication and other related effects. We have first performed calculations for GaAs as a standard material and compare our results for the drift velocity, the mean kinetic energy, and the valley occupation with experiments and other simulations; a very good agreement can be stated. New *ab initio* results are then shown for the wide band gap material ZnS where a strong influence of the band structure on the transport properties is evident. This underlines the need to use realistic band structures in full band Monte Carlo simulations of high field electron transport as presented here within the EXX-LDA schema. Work for GaN and SrS is in progress.

Band structures.– We have performed electron structure calculations using DFT within the EXX-LDA as outlined in Refs. [5, 6]. This approximation treats a local Kohn-Sham exchange potential V_x exactly, while the correlation contributions are considered using the LDA Perdew-Zunger parameterization [7] based on a quantum Monte Carlo simulation of Ceperley and Alder [8]. All calculations use consistent norm-conserving Troullier-Martins-type EXX-LDA pseudopotentials [9] in the Kleinman-Bylander form [10]. We use energy cutoffs of 23 Ry for GaAs and 60 Ry for ZnS and all calculations were carried out at the experimental lattice constants. The band structure is calculated at 916 points in the irreducible wedge of the Brillouin zone. In addition, for the density of states we use 2573 points as input for the Monte Carlo simulations. The 3d electrons of Zn were treated as part of the frozen core.

TABLE I: Comparison of band gaps in GaAs and ZnS calculated with the present EXX-LDA and the EPM method (GaAs: Ref. [17], ZnS: Ref. [20].

	L		Γ		X	
	EXX	EPM	EXX	EPM	EXX	EPM
GaAs	2.60	2.58	1.40	1.43	4.27	4.02
ZnS	5.19	5.60	3.74	3.73	5.82	6.58

The EXX-LDA *ab initio* band structures provide a new reference for those materials for which only few experimental data exist and where the use of the empirical pseudopotential method (EPM) leads to relatively great uncertainties. For instance, recent EXX-LDA calculations have shown that ScN [11] and SrS [12] are both semiconductors with an indirect $\Gamma - X$ band gap of 1.3 eV (ScN) and 3.71 eV (SrS), respectively.

The resulting band structures and densities of states (DOS) are shown in Fig. 1 for GaAs and in Fig. 2 for ZnS. The results for GaAs coincide with those reported earlier by Städele *et al.* [6] while those for ZnS are presented here for the first time. Fundamental band gaps are tabulated in Table I for both materials and are compared with the respective EPM data. The sets of EPM parameters used in this work for GaAs can be found in [13] and for ZnS in [14], respectively.

Previous EPM calculations for GaAs [15–17] are in very good overall agreement with the EXX-LDA results shown in Fig. 1 which is to be seen from Table I for the band gaps at special points so that the use of empirical pseudopotentials is well founded for GaAs. This is not the case for ZnS where deviations between the EPM band structures as used, e.g., in Refs. [17–20] and the present EXX-LDA occur, even for the lowest conduction band and the highest valence band. Especially, the band gaps of the EXX-LDA calculations at the L and X point are substantially smaller than those of the EPM which is of importance for higher field strengths where these valleys will be occupied. The same arguments apply for the DOS.

Ensemble Monte Carlo simulations.– We use the band structures shown in Figs. 1 and 2 and the densities of states above the bottom of the conduction bands within ensemble Monte Carlo (EMC) simulations to study the high field transport in both materials. The EMC method has been explained in detail elsewhere [3, 19, 20]. Discretization in the Brillouin zone was chosen to be $\Delta k = 0.05\ 2\pi/a$ so that a total of 33861 points is considered in the simulations.

We consider an ensemble of 64.000 electrons in an external electrical field. The scattering processes are treated by a Monte Carlo method at every time step of $\Delta t = 10$ fs for GaAs and $\Delta t = 2$ fs for ZnS . The total

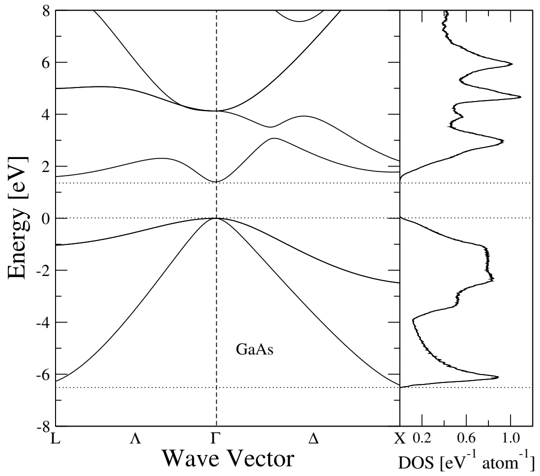

FIG. 1: Band structure and density of states for GaAs using DFT in EXX-LDA.

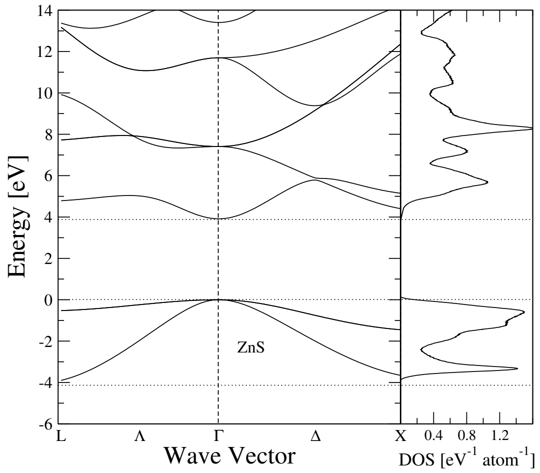

FIG. 2: Band structure and density of states for ZnS using DFT in EXX-LDA.

simulation time is 10 ps for GaAs and 0.8 ps for ZnS. The average is performed over the steady final state which is reached after about 80% of the simulation time.

We take into account the electron-phonon scattering (acoustic and optical nonpolar scattering, polar optical scattering via the Fröhlich interaction, nonpolar intervalley scattering, and ionized impurity scattering via the Conwell-Weisskopf formula; for details, see Refs. [15, 16]) as well as inelastic electron-electron scattering (impact ionization; for details, see Refs. [13, 21]).

The resulting drift velocity $\langle v_D \rangle$, average energy $\langle E \rangle$, and valley occupations in GaAs are shown in Figs. 3-5, respectively, as function of the applied electrical field strength. We compare the drift velocity with experimental data [22] and other simulations [15–17] which use an EPM band structure and the relevant scattering mechanisms as in the present work.

For both quantities, the agreement between simulation

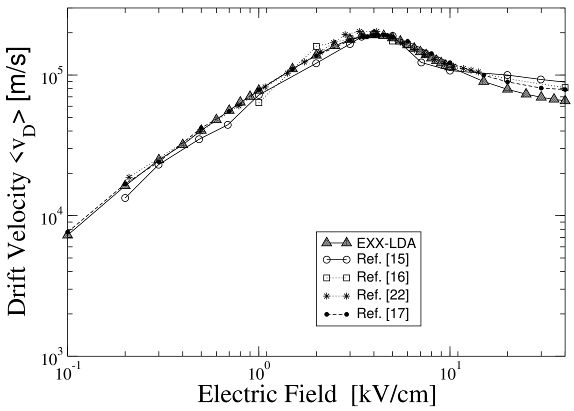

FIG. 3: Drift velocity in GaAs at 300 K using the band structure derived from DFT within EXX-LDA. Results from previous Monte Carlo simulations using an EPM band structure [15–17] and experimental results [22] are also shown.

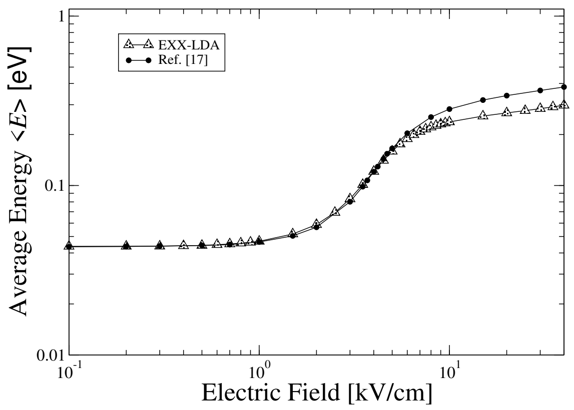

FIG. 4: Average energy $\langle E\rangle$ for GaAs derived from DFT within EXX-LDA compared with previous Monte Carlo simulations using an EPM band structure [17].

results using the EPM and EXX-LDA band structures is very good below 10 kV/cm as can be expected from the coincidence of the band structures itself. For higher field strengths, the drift velocities derived from the EXX-LDA band structure are systematically smaller than the respective EPM results. The same trend is to be seen for the average energies but already above 7 kV/cm. This corresponds to the occupation of the different valleys, see Fig. 5. In this region the occupation of the L valley sets in at the expense of the Γ valley; the effect is more pronounced using the EXX-LDA band structure than the EPM results. The occupation of the X valley is almost the same using both data sets and important only for high field strengths above 100 kV/cm.

The drift velocity, average energy, and valley occupation in ZnS are shown as function of the field strength in Figs. 6-8, respectively. The EXX-LDA results for the drift velocity are smaller than previous EPM calculations in the field range up to 150 kV/cm [17]. We show

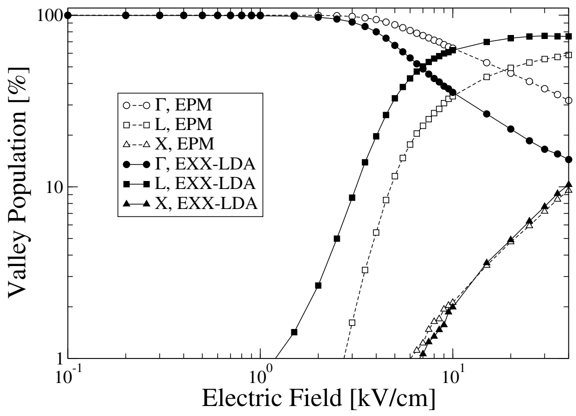

FIG. 5: Valley occupation in GaAs: The EXX-LDA results are compared with those using an EPM band structure [17].

also standard reference data for the drift velocity [23] as shaded area which lies between both curves. The maximum drift velocity in the EPM study occurs at about 100 kV/cm [17] compared with 200 kV/cm in the present EXX-LDA calculation. These discrepancies are obviously due to different effective masses which can be derived from both band structure calculations. For instance, we get effective masses in the Γ valley of 0.178 m_0 from the EPM and of 0.342 m_0 from the EXX-LDA. The latter result agrees perfectly with the value of 0.34(2) m_0 derived from infrared absorption measurements [24]. Saturation occurs at high field strengths at about the same values than obtained in the EPM calculation. The drift velocities reported by Brennan [18] within another EPM calculation are substantially higher than those shown in Fig. 6 because ionized impurity scattering was not included.

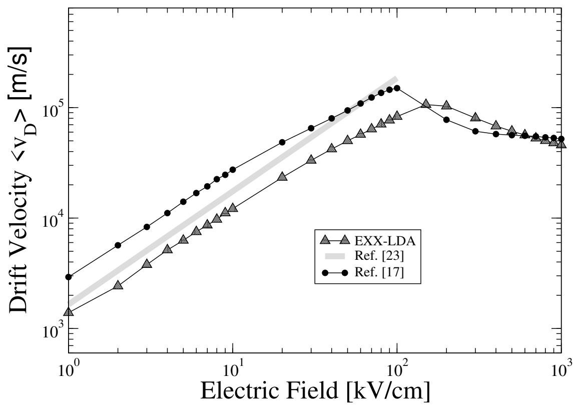

FIG. 6: Drift velocity in ZnS at 300 K using the band structure derived from DFT within EXX-LDA. Results from previous Monte Carlo simulations using an EPM band structure [17] and experimental data from [23] are shown for comparison.

The average energy shows a strong increase above 50 kV/cm (EPM) and 80 kV/cm (EXX-LDA), see Fig. 7. This behavior originates from the occupation of the

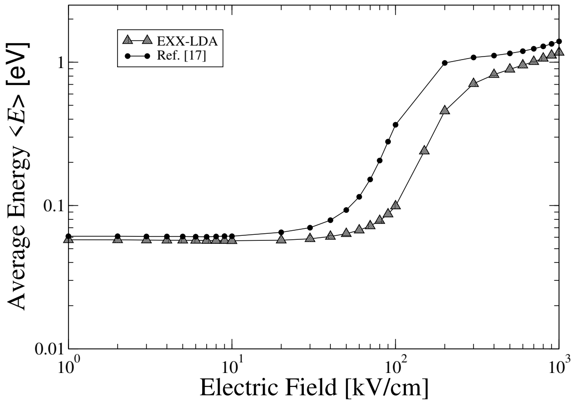

FIG. 7: Average energy $\langle E\rangle$ for ZnS derived from DFT within EXX-LDA compared with a previous Monte Carlo simulation using an EPM band structure [17].

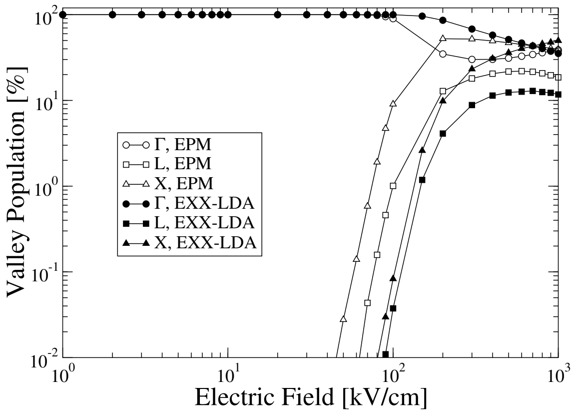

FIG. 8: Valley occupation in ZnS: The EXX-LDA results are compared with those using an EPM band structure [17].

neighboring valleys which starts above 100 kV/cm, see Fig. 8. The EXX-LDA results show a slightly retarded occupation of the X and L valley compared with the EPM and remain at values of about 30-40% (X) and 10% (L) for high field strengths. There the EPM shows a decrease and a reoccupation of the Γ valley. As a result, the average energy is always higher in the EPM than in the EXX-LDA calculation.

Conclusions.– We have performed *ab initio* band structure calculations for GaAs and ZnS using DFT within the EXX-LDA. Ensemble Monte Carlo simulations were performed to study electron transport in these bulk materials, especially in the high field regime. All relevant scattering mechanisms including impact ionization were considered. For GaAs, a very good agreement with experimental data is found and previous calculations using standard EPM band structures are verified. For ZnS, the first use of an *ab initio* EXX-LDA band structure for simulations of electron transport has lead to modified results for the drift velocity and the mean kinetic energy. The drift velocity is smaller than derived from the EPM, has its maximum (10^5 m/s) at higher field strengths of about 200 kV/cm, and saturates at values of about 4×10^4 m/s.

Acknowledgements.– This work was supported by the Deutsche Forschungsgemeinschaft under contracts No. Re 882/9-2 and Scha 360/17-2.

[1] *Quantum Transport in Semiconductors*, edited by C. Jacoboni, L. Reggiani, and D. K. Ferry (Plenum Press, New York, 1992).
[2] K. Brennan, J. Appl. Phys. **64**, 4024 (1988).
[3] K. Bhattacharyya, S. M. Goodnick, and J. F. Wager, J. Appl. Phys. **73**, 3390 (1993).
[4] K. Kometer, G. Zandler, and P. Vogl, Phys. Rev. B **46**, 1382 (1992).
[5] M. Städele, J. A. Majewski, P. Vogl, and A. Görling, Phys. Rev. Lett. **79**, 2089 (1997).
[6] M. Städele, M. Moukara, J. A. Majewski, P. Vogl, and A. Görling, Phys. Rev. B **59**, 10031 (1999); see also J. P. Perdew and M. Levy, Phys. Rev. Lett. **51**, 1884 (1983), L. J. Sham and M. Schlüter, Phys. Rev. Lett. **51**, 1888 (1983).
[7] J. P. Perdew and A. Zunger, Phys. Rev. B **23**, 5048 (1981).
[8] D. M. Ceperley and B. I. Alder, Phys. Rev. Lett. **45**, 566 (1980).
[9] N. Troullier and J. L. Martins, Phys. Rev. B **43**, 1993 (1991); **43**, 8861 (1991).
[10] L. Kleinman and D. M. Bylander, Phys. Rev. Lett. **48**, 1425 (1982).
[11] D. Gall, M. Städele, K. Järrendahl, I. Petrov, P. Desjardins, R. T. Haasch, T.-Y. Lee, and J. E. Greene, Phys. Rev. B **63**, 125119 (2001).
[12] N. Fitzer, PhD thesis (University of Rostock, 2002), unpublished.
[13] M. Stobbe, R. Redmer, and W. Schattke, Phys. Rev. B **49**, 4494 (1994).
[14] M. Reigrotzki, R. Redmer, N. Fitzer, S. M. Goodnick, M. Dür, and W. Schattke, J. Appl. Phys. **86**, 4458 (1999).
[15] M. V. Fischetti and S. E. Laux, Phys. Rev. B **38**, 9721 (1988).
[16] G. M. Dunn, G. J. Rees, J. P. R. David, S. A. Plimmer, and D. C. Herbert, Semiconductor Science and Technology **12**, 111 (1997).
[17] M. Reigrotzki, PhD thesis (University of Rostock, 1998), unpublished.
[18] K. F. Brennan, J. Appl. Phys. **64**, 4024 (1988).
[19] M. Reigrotzki, R. Redmer, I. Lee, S. S. Pennathur, M. Dür, J. F. Wager, S. M. Goodnick, P. Vogl, H. Eckstein, and W. Schattke, J. Appl. Phys. **80**, 5054 (1996).
[20] M. Dür, S. M. Goodnick, S. S. Pennathur, J. F. Wager, M. Reigrotzki, and R. Redmer, J. Appl. Phys. **83**, 3176 (1998).
[21] M. Reigrotzki, M. Stobbe, R. Redmer, and W. Schattke, Phys. Rev. B **52**, 1456 (1995).
[22] J. G. Ruch and G. S. Kino, Phys. Rev. **174**, 921 (1968).
[23] O. Madelung (Editor), *New Series III/22a Landolt-Börnstein* (Springer, Berlin, 1987), p. 167.
[24] H. Kukimoto, S. Shionoya, T. Koda, T. Hioki, J. Phys. Chem. Sol. **29**, 935 (1968).